Seasonal and diurnal variations of biogenic volatile organic compounds in highland and lowland ecosystems in southern Kenya

Yang Liu[1], Simon Schallhart[2], Ditte Taipale[3], Toni Tykkä[2], Matti Räsänen[3], Lutz Merbold[4,+], Heidi Hellén[2], Petri Pellikka[1,3]

[1] Department of Geosciences and Geography, University of Helsinki, P.O. Box 64, 00014 Helsinki, Finland

[2] Finnish Meteorological Institute, PL 503, 00101 Helsinki, Finland

[3] Institute for Atmospheric and Earth System Research / Physics, Faculty of Science, University of Helsinki, P.O. Box 64, 00014 Helsinki, Finland

[4] Mazingira Centre, International Livestock Research Institute, P.O. Box 30709, 00100 Nairobi, Kenya;

[+] now at Agroscope, Research Division Agroecology and Environment, Reckenholzstrasse 191, 8046, Zurich, Switzerland

Correspondence: Yang Liu (yang.z.liu@helsinki.fi)

Abstract. The East African lowland and highland areas consist of water-limited and humid ecosystems. The magnitude and seasonality of biogenic volatile organic compounds (BVOCs) emissions from these functionally contrasting ecosystems are limited due to a scarcity of direct observations. We measured mixing ratios of BVOCs from two contrasting ecosystems, humid highlands with agroforestry and dry lowlands with bushland, grassland, and agriculture mosaics, during both the rainy and dry seasons of 2019 in southern Kenya. We present the diurnal and seasonal characteristics of BVOC mixing ratios and their reactivity, and estimated emission factors (EFs) for certain BVOCs from the African lowland ecosystem based on field measurements. The most abundant BVOCs were isoprene and monoterpenoids (MTs), with isoprene contributing > 70 % of the total BVOC mixing ratio during daytime, while MTs accounted for > 50 % of the total BVOC mixing ratio during nighttime at both sites. The contributions of BVOCs to the local atmospheric chemistry were estimated by calculating the reactivity towards the hydroxyl radical (OH), ozone (O_3), and the nitrate radical (NO_3). Isoprene and MTs contributed the most to the reactivity of OH and NO_3, while sesquiterpenes dominated the contribution of organic compounds to the reactivity of O_3.

The mixing ratio of isoprene measured in this study was lower to that measured in the relevant ecosystems in west and south Africa, while that of monoterpenoids was similar. Isoprene mixing ratios peaked daily between 16:00 and 20:00 with a maximum mixing ratio of 809 parts per trillion by volume (pptv) and 156 pptv in the highlands, and 115 pptv and 25 pptv in the lowlands, during the rainy and dry seasons, respectively. MT mixing ratios reached their daily maximum between midnight and early morning (usually 04:00 to 08:00) with mixing ratios of 254 pptv and 56 pptv in the highlands, and 89 pptv and 7 pptv in the lowlands, in the rainy and dry seasons, respectively. The dominant species within the MT group were limonene, α-pinene, and β-pinene.

EFs for isoprene, MTs, and 2-methyl-3-buten-2-ol (MBO) were estimated using an inverse modeling approach. The estimated EFs for isoprene and β-pinene agreed very well with what is currently assumed in the world's most extensively used biogenic emissions model, the Model of Emissions of Gases and Aerosols from Nature (MEGAN), for warm C4 grass, but the estimated EFs for MBO, α-pinene, and especially limonene, were significantly higher than that assumed in MEGAN for the relevant plant functional type. Additionally, our results indicate that the EF for limonene might be seasonally dependent in savanna ecosystems.

1 Introduction

Biogenic volatile organic compounds (BVOCs) are emitted from vegetation during, e.g., plant growth (e.g., Hüve et al.,
40 2007; Aalto et al., 2014; Taipale et al., 2020), reproduction (e.g., Andersson et al., 2002; Wright et al., 2005), and for
defense (Niinemets, 2010; Holopainen and Gershenzon, 2010; Faiola and Taipale, 2020). The reactions of BVOCs with
the hydroxyl radical (OH), nitrate radical (NO_3), and ozone (O_3) (Schulze et al., 2017; Ng et al., 2017) contribute to the
oxidation capacity of the atmosphere (e.g., Mogensen et al., 2015), produce less volatile compounds which can form and
growth atmospheric clusters (Matsunaga et al., 2005; Ehn et al., 2014; Kulmala et al., 2006), and impact cloud
45 condensation and scattering of solar radiation, affecting biosphere–atmosphere interactions and local/regional climate
change (Claeys et al., 2004; Peñuelas and Staudt, 2010; Sporre et al., 2019) (Fig. 1).

Climate change affects BVOC emissions and oxidation through environmental conditions (Fig. 1: red arrows).
Isoprene emissions are known to be both temperature and light dependent (Guenther et al., 1991, 1993; Wildermuth and
Fall, 1996; Niinemets et al., 2004) and have been identified as the main contributor to increasing global BVOC levels in
50 response to global warming (Peñuelas and Staudt, 2010). Besides temperature and light, the emission of isoprene depends
on soil water availability and thus responds to soil water stress (Guenther et al., 2012). The emission of monoterpenes is
known to mainly be controlled by temperature, but the emission of certain monoterpenes (e.g., ocimene) depends greatly
on the availability of light (Jardine et al., 2015; Guenther et al., 2012; Loreto et al., 1998). Mochizuki et al. (2020)
estimated that monoterpene emissions will increase by 15 % with a 1 °C increase in air temperature due to climate
55 warming. The emission of certain monoterpenes is promoted by increasing soil moisture (Schade et al., 1999; Greenberg
et al., 2012) and a decline in moisture–limited conditions (Bonn et al., 2019). Increasing atmospheric carbon dioxide
(CO_2) and air pollution (e.g., O_3) are also abiotic factors which affect BVOC emissions negatively or positively (Velikova,
2008; Masui et al., 2021). Since climate variability is rising (Seneviratne et al., 2012), the emission of monoterpenes and
isoprene is becoming more variable. This effect becomes especially pronounced in ecosystems that are vulnerable to
60 climatic changes.
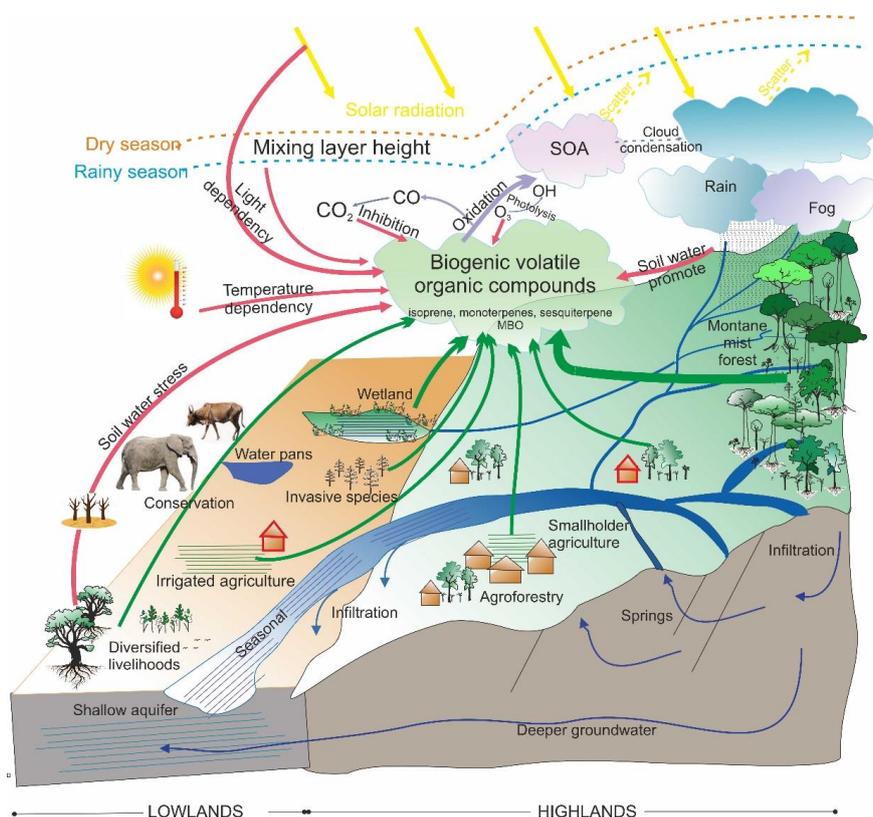
Figure 1. Atmospheric oxidation and abiotic effects on biogenic volatile organic compounds (BVOCs) in African highland and lowland ecosystems. The ecosystem impacts on CO_2 concentration (e.g. photosynthesis and respiration) are not shown in the figure above. SOA: secondary organic aerosol, OH: hydroxyl radical. The green arrows indicate BVOC
65 sources from African ecosystems. BVOC oxidation and products are shown as purple arrows. The dashed yellow and purple arrows mean BVOC indirect impact to the climate. The abiotic effects on BVOC emissions are shown as red arrows. Blue arrows mean rivers and groundwater. The environments of our study areas are shown as the red house symbols.

Dryland ecosystems and human-modified systems, including savannas, bushland, grassland, and agroforestry are more
70 sensitive and vulnerable to ongoing climate change than other ecosystems (IPCC, 2014). It is estimated that around 18 % of global BVOCs are emitted from grass, shrubs, and crops (Guenther, 2013). This estimate is unfortunately connected with a large degree of uncertainty, since BVOC measurements from these ecosystems are rather scarce (e.g., Guenther et al., 2013). These climate–sensitive ecosystems are widely distributed and cover 55.2 % of tropical Africa (MDAUS BaseVue 2013, https://www.africageoportal.com/datasets/b4a808eba17d4294991880d9e120faee, last access: December
75 15, 2020), which have high potential on native ecosystem changes (Zabel et al., 2019), e.g. human-modified systems expansion at the expense of grassland and savannas, which can decrease the global BVOC levels (Unger, 2014). However, these aforementioned climate–sensitive ecosystems are also estimated to face a higher frequency of heat waves, hot nights, droughts, and flooding in the future climate (Niang et al., 2014; Kharin et al., 2018), which can promote or inhibit the certain BVOC releases and make BVOC emissions more changeable. Models can simulate certain abiotic effects, for

80 example temperature changes, soil water stress, and CO_2 inhibition, on BVOC emissions from these climate–sensitive ecosystems in current and future climate scenarios through the setting of suitable parameterizations, i.e., emission factors (EFs) and activity factors (Guenther et al., 2012; Emmerson et al., 2020). However, field measurements focusing on volatile organic compounds (especially on monoterpenoids (MTs), sesquiterpenes (SQTs), and 2-methyl-3-buten-2-ol (MBO)) from African ecosystems are very limited. Previous measurements in tropical savannas have mainly focused on

85 isoprene and/or monoterpenes (Guenther et al., 1996; Klinger et al., 1998; Greenberg et al., 1999, 2003; Otter et al., 2002; Harley et al., 2003; Stone et al., 2010; Jaars et al., 2016; Liu et al., 2021) (Figure 1: green arrows), and were measured during the local rainy season (except Jaars et al., 2016), which increases the challenge of BVOC estimation in these climate–sensitive African ecosystems.

Thus, the overall objective of this study was to quantify BVOC mixing ratios in the humid highland dominated by

90 agroforestry, and the dry lowlands with bushland and agriculture mosaic landscapes in Kenya during the rainy and dry season of 2019. We hypothesized considerable differences in BVOC mixing ratios between land cover type, at diurnal scale and at season scale. We interested in the diurnal as well as the seasonal variation in BVOC mixing ratios, and we estimated EFs for BVOCs to improve the representation of BVOC emissions from African ecosystems in models.

2 Material and methods

95 ### 2.1 Experimental sites in Taita Taveta County

BVOC mixing ratios and meteorological measurements were set up in Taita Taveta County in southern Kenya. The county consists of dry savannas located in the lowlands between 500 and 1000 m a.s.l., and highlands ranging from approximately 1100 to 2200 m a.s.l. (Pellikka et al., 2018).

Taita Taveta County has two rainy and two dry seasons annually due to the Intertropical Convergence Zone forming a

100 bimodal rainfall pattern. The first rainy season (often referred to as the long rains) occurs between March and June, while the second rainy season (referred to as the short rains) is between October and December. The two rainy seasons are separated by dry seasons, with a short hot and dry season from January to February and a long cool and dry season from June to September (Ayugi et al., 2016; Wachiye et al., 2020). The highlands receive more rainfall than the lowlands. The annual precipitation is on average 1132 mm in Mgange (1768 m a.s.l.), corresponding to about twice the rainfall received

105 in Voi at 560 m a.s.l. (587 mm) (Erdogan et al., 2011). The annual temperature is 18.5 °C in Taita Research Station in the highlands and 22.3 °C in Maktau field site in the lowlands between 2013 and 2021. Both meteorological measurements are managed by the University of Helsinki, Finland. The length of sunlight remains 12 ± 0.5 hour through the entire year, with sunrise around $06:00 \pm 0.5$ hour and sunset about $18:00 \pm 0.5$ hour depending on the season (all times are given as East Africa Time, UTC +3).

110 The experimental sites were set up in the highlands in Wundanyi at Taita Research Station of the University of Helsinki and in the lowlands in the Maktau field site to represent the highland and lowland ecosystems, respectively (Fig. 2). The Taita Research Station (3° 40′ S, 38° 36′ E; 1415 m) is located in the middle of the Taita Hills on a windward slope. The landscape is characterized by small agricultural fields with a variety of crops, such as maize, beans, avocados, and grass, with small native or exotic forest stands. The measurement station, which is fenced off, is surrounded by agroforestry

115 landscape, with the closest native and exotic forests at 200 m distance. The natural ecosystem of the Wundanyi site is humid montane forest (Pellikka et al., 2009). Broadleaf evergreen trees and lush grass covered the ground layer during the rainy season at the Wundanyi site (Fig. 2b), while part of the leaves were shed from trees and grass was dried out

around our instrument during the dry season (Fig. 2c). The Maktau field site (3° 25′ S, 32° 74′ E; 1056 m) is located in the lowlands in which the natural ecosystem would be Acacia-commiphora bushland on savanna (Amara et al., 2020).

120 The measurement site is located inside a fenced farm growing maize, cassava, beans, and papaya trees, surrounded by bushland. The soil on this site was not ploughed yet and field was not sown or re-planted during our rainy season measurements (Fig. 2d). The instrument was positioned near young cassava bush, with a distance of 50 m from the nearest bushland edge. In the dry season, we collected the samples two weeks after the maize was harvested, the dry maize residuals still remaining on the ground (Fig. 2e). The bushland surrounding the field was almost leafless during the dry

125 season sampling, while during the rainy season sampling, the new leaves were starting to sprout. The sites were chosen for two reasons: 1) they represented typical highland agroforestry and lowland dry agriculture ecosystems with typical bushland and forest cover, and 2) they provided safety and electricity for continuous measurements.
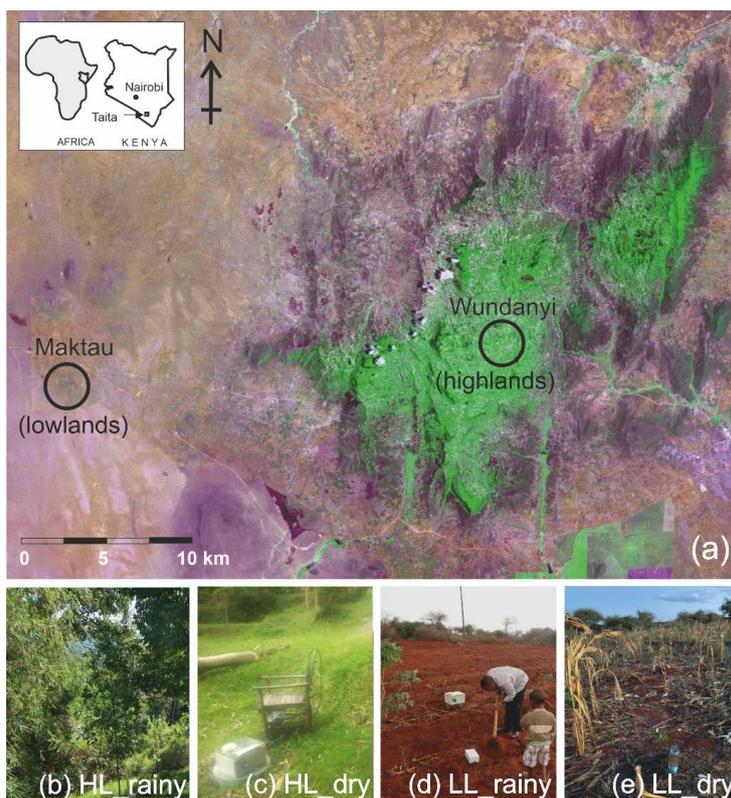
Figure 2. Locations of the highland site (HL) in Wundanyi and the lowland site (LL) in Maktau. Green color in the true

130 color Sentinel satellite image (a) shows the forests and agricultural area in Taita Hills, while magenta represents grassland with a few fire scars. The brownish areas are areas with less land cover, such as dry bushland, dryland agriculture, and areas used for livestock management. Photographs (b, c, d, e) show the phenological conditions and the surrounding environments of the measurement sites during sampling in the rainy season in April and dry season in September.

2.2 Sample collection and chemical analysis of BVOC mixing ratios

135 We conducted four campaigns, each lasting several days, in the highlands and lowlands during the onset of the rainy season from April 10 to 17, 2019 and during the dry season from September 1 to 19, 2019 (Table A1).

The measurements took place upwind of the two sites, away from roads and at least 10 m away from the nearest residential buildings. Two autosamplers were used to collect air into thermal desorption sorbent tubes (STS 25, PerkinElmer, Waltham, MA, USA), with a flow rate of 100 standard cubic centimeters per minute. All tubes were filled 140 with Tenax TA (60/80 mesh, Sigma-Aldrich, St. Louis, MO, USA) and Carbopack B (60/80 mesh, Sigma-Aldrich, St. Louis, MO, USA). The sampling time was generally 4 hours but was only 2 hours during the second campaign due to frequent power failures (Table A1). The sampling took place 25 cm above the ground so that flowing water during heavy rainfall events did not disturb the measurements.

The mixing ratios of isoprene (C_5H_8), MBO ($C_5H_{10}O$), MTs ($C_{10}H_{16}$ and $C_{10}H_{18}O$), SQTs ($C_{15}H_{24}$), and bornyl acetate 145 ($C_{12}H_{20}O$) were measured. MTs consisted of α-pinene, β-pinene, limonene, 3Δ-carene, ρ-cymene, camphene, terpinolene, linalool, and 1,8-cineol. SQTs consisted of longicyclene, iso-longifolene, β-caryophyllene, β-farnesene, and α-humulene. All samples were analyzed in the laboratory of the Finnish Meteorological Institute. An automatic thermal desorption device (PerkinElmer TurboMatrix 650) was connected to a gas chromatograph (PerkinElmer Clarus 600) with a DB-5MS column (50 m × 0.25 mm, film 0.5 μm) and a mass-selective detector (PerkinElmer Clarus 600T). We desorbed all sample 150 tubes at 300 °C for 5 minutes before cryo-focusing the samples in a Tenax TA cold trap (−30 °C) and injecting them into the column by rapidly heating the cold trap to 300 °C. The method has been described in detail in Helin et al. (2020).

Standards in methanol solutions were used to calibrate the MBO, MTs, and SQTs. We injected the standards into the sampling tubes and flushed away the methanol for 10 minutes before the analysis. The gaseous calibration standard (National Physical Laboratory) was applied for isoprene. Calibration samples were analyzed together with real samples.

2.3 Complementary measurements and oxidant estimation

2.3.1 Meteorological data

Meteorological data were measured simultaneously with sampling of BVOCs at Taita Research Station and Maktau Weather Station. Hourly air temperature (CS215, Campbell Scientific, UK), relative humidity (CS215, Campbell Scientific, UK), precipitation (ARG100, EML, UK), wind speed and direction (Taita: Wind monitor 05103, R. M. Young, 160 Traverse City, MI, USA; Maktau: 03002-L Wind Sentry Set, R. M. Young, Traverse City, MI, USA) were measured at both stations. All instruments were positioned at 1.5 m above the ground. Atmospheric pressure (CS106 Barometric pressure sensor, Vaisala, Finland), photosynthetic photon flux density (PPFD) (SKP215 Quantum, Skye Instruments, UK), and soil moisture (CS650 sensor, Campbell Scientific, UK) were additionally measured at Maktau. PPFD sensor was positioned around 4 m above the ground. Soil moisture was measured depths of 10 and 30 cm. Root–zone soil 165 moisture calculation has been described in Räsänen et al. (2020).

The Chemistry Land–surface Atmosphere Soil Slab model was used to estimate mixing layer heights (MLHs) at the lowland site (Python version, Vilà-Guerau de Arellano et al., 2015). The model initial conditions were derived from the weather station observations. The sensible and latent fluxes from eddy covariance measurements were used as model input. These flux measurements were corrected by conserving the Bowen ratio using the net radiation measurements 170 (Combe et al., 2015). The diurnal MLH data start from 06:00 and continue to 18:00, and the MLHs ranged from 337 ± 25 m to 2539 ± 197 m during the rainy season campaign in April, and from 361 ± 18 m to 2755 ± 146 m during the dry season campaign in September. All meteorology data during BVOC measurements are showed in Fig. 3.
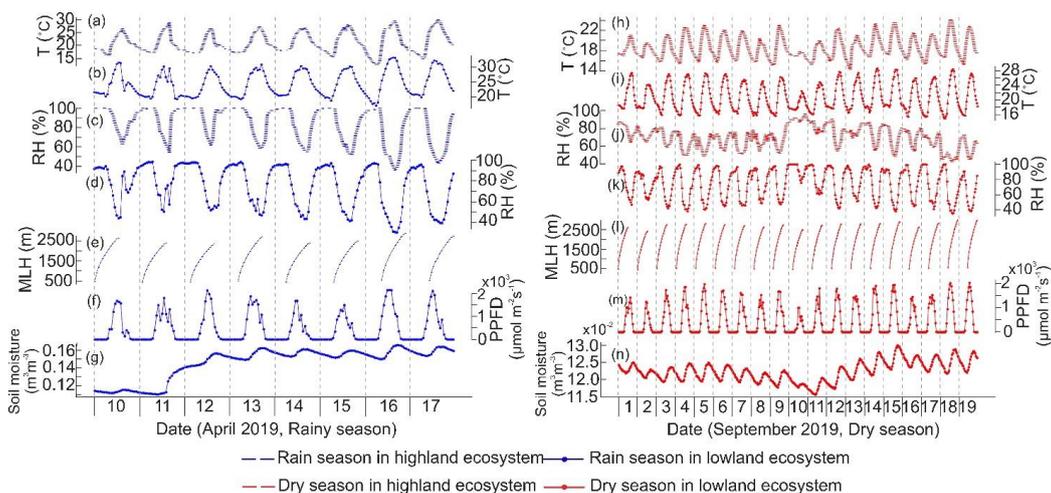
Figure 3. Meteorological measurements in the highland and lowland ecosystems during the rainy and dry seasons. **(a, h)** air temperature (T) in the highlands, **(b, i)** T in the lowlands, **(c, j)** relative humidity (RH) in the highlands, **(d, k)** RH in the lowlands, **(e, l)** mixing layer height (MLH) in the lowlands, **(f, m)** photosynthetic photon flux density (PPFD) in the lowlands, **(g, n)** soil moisture in the lowlands.

2.3.2 Oxidant concentration estimation

Since the concentrations of oxidants were not measured directly during the campaigns, we used data observed by an Ozone Monitoring Instrument to acquire O_3 column densities to estimate O_3 concentrations (the conversion method is described at WDC, http://wdc.dlr.de/data_products/SERVICES/PROMOTE_O3/vmr.html, last access: December 15, 2020) and ultraviolet B (UVB) radiation intensity to calculate OH radical proxies using Eq. 1 (Rohrer et al., 2006; Petäjä et al., 2009).

$$OH_{proxy} = 5.62 \times 10^5 \times UVB^{0.62} \qquad (1)$$

The calculated average midday (local noon time) concentrations of O_3 were 31 parts per billion by volume (ppbv) and 29 ppbv in the rainy and dry seasons, respectively, while the corresponding concentration of OH was estimated to be 1.2×10^6 and 1.1×10^6 molecule cm^{-3} in the rainy and dry seasons in our study area, respectively.

2.4 Reactivity calculation

Calculating the reactivity of BVOCs gives insight into the relative role of BVOCs in local atmospheric chemistry. The reactivity of BVOCs ($R_{i,x}$, where i refers to the BVOC species and x the oxidant species) was calculated by multiplying the mixing ratio of a specific BVOC (i) with the corresponding reaction rate coefficient ($k_{i,x}$) of oxidants (including O_3, OH, NO_3) using Eq. 2.

$$R_{i,x} = BVOC_i \times k_{i,x} \qquad (2)$$

The parameter $k_{i,x}$ was calculated by using the average air temperature during each measurement (calculation equations described in Table A2). All of the reaction rate coefficients used in this study are provided in Table A3.

The atmospheric lifetime (τ) of different BVOCs shows the oxidation speed of a specific compound or compound group in the atmosphere (Eq. 3). We calculated the lifetime of measured BVOCs in relation to O_3 and OH (x), as stated in Table A3.

$$\tau_{i,x} = \frac{1}{m}\sum_m (k_{i,x} \times Oxidant_x)^{-1} \qquad (3)$$

200   The amount of measurements in a certain period (m) was used to average over different measurement periods described hereafter as late night (00:00 to 04:00), early morning (04:00 to 08:00), late morning (08:00 to 12:00), early afternoon (12:00 to 16:00), late afternoon (16:00 to 20:00), and early night (20:00 to 00:00).

2.5 Emission factor estimation

EFs were estimated for isoprene, MBO, and the detected MTs using inverse modeling. In practice, a simple BVOC
205   emissions and chemistry model was developed for this purpose. The model includes an emissions module based on Guenther et al. (2012). The emissions (F_i) of BVOCs (i) are calculated as $F_i = \gamma_i \cdot EF_i$, where γ_i (Eq. 2 in Guenther et al., 2012) is an activity factor which accounts for emission responses due to various environmental parameters and phenological conditions. We considered BVOC emission responses due to light (Eq. 3-6 in Guenther et al., 2012), temperature (Eq. 7-11 in Guenther et al., 2012), and soil moisture (Eq. 13a-c in Guenther et al., 2012). A value of 0.57
210   was assigned to the canopy environment coefficient (C_{CE}) (Simpson et al., 1999, 2012; Guenther et al., 2012), while the one-sided   leaf   area   index   (LAI,   obtained   from   PROBA-V,   spatial   resolution   300 m, https://land.copernicus.eu/global/products/lai, last access: December 14, 2020) was kept constant at a value of 1.53 m^2 m^{-2} (April) or 0.3 m^2 m^{-2} (September). The model's chemistry module consists of the first step in the oxidation of the BVOCs by O_3 and OH using the reaction rate coefficients listed in Table A2. Reactions with NO_3 were omitted,
215   because simulations were only carried out using day time observations. The model takes the following parameters as input: observations of air temperature, PPFD, and soil moisture from the Maktau site, estimated concentrations of O_3 and OH (Section 2.3.2), modeled daytime MLHs (Section 2.3.1), leaf temperatures calculated from observed air temperatures (Eqs 14.2 to 14.6 in Campbell et al., 1998), and LAI. In the model, the concentration of O_3 is kept constant within a day, while the daily pattern of the OH concentration follows the solar zenith angle.

220   Initial estimations were made for the EFs, and the mixing ratios of the BVOCs were predicted using the model for one campaign day at a time. The predicted and measured daytime BVOC mixing ratios were then compared (2–5 data points per day) and the sum of the squared differences between the predicted and observed mixing ratios was calculated for each individual BVOC for each day. A new estimation for the values of the EFs was made and the process was iterated until a minimum sum of the squared differences was obtained. The EF, for each individual BVOC, which led to this
225   minimum value, was considered the most appropriate value for the EF for that particular day. Similar simulations were conducted for each measured day. The median values of the estimated EFs during either the rainy or dry season, for each individual BVOC, are our best estimates for the BVOC EFs for the agriculture site located in the savanna ecosystem at Maktau field site.

3 Results and discussion

230   **3.1 Seasonal and diurnal variations of BVOC mixing ratios**

For most of the compounds studied, the daily mean mixing ratio was higher during the rainy season than during the dry season. The daily mean isoprene mixing ratio ranged from 134 to 442 pptv in the highlands and from 22 to 69 pptv in the lowlands in the rainy season. The daily mean mixing ratio of MTs was 117 to 233 pptv in the highlands and 29 to 96 pptv in the lowlands, and that of SQTs was 2 to 30 pptv in the highlands and 1 to 2 pptv in the lowlands during the rainy season. During the dry season, the isoprene mixing ratio ranged from 36 to 150 pptv in the highlands and from 6 to 15 pptv in the lowlands. The mixing ratio of MTs ranged from 8 to 75 pptv and 3 to 9 pptv, while the mixing ratio of SQTs ranged from 1 to 3 pptv and was less than 1 pptv, in the highlands and lowlands, respectively, during the dry season.

3.1.1 Mixing ratios of isoprene and monoterpenoids

Isoprene and MTs explained over 88 % of the total BVOC mixing ratios of all collected samples, and their mixing ratios in the rainy season were higher than in the dry season in both the highlands and lowlands. The seasonal mean ± standard deviation of the isoprene mixing ratio was 252.2 ± 285 pptv and 55.3 ± 56 pptv in the rainy season in the highlands and the lowlands, respectively, while the corresponding values were 145.5 ± 73 pptv and 57.8 ± 46 pptv for MTs (Fig. 4). During the dry season, the mixing ratio of isoprene was 66.6 ± 75 pptv and 11.2 ± 9 pptv in the highlands and the lowlands, respectively, while the corresponding values for MTs were 35.2 ± 42 pptv and 4.1 ± 4 pptv. Isoprene and all the MTs (except 1,8-cineol) showed a clear mixing ratio maximum in the rainy season, and the seasonal mixing ratios of isoprene and MTs remained lower in the lowlands than in the highlands.
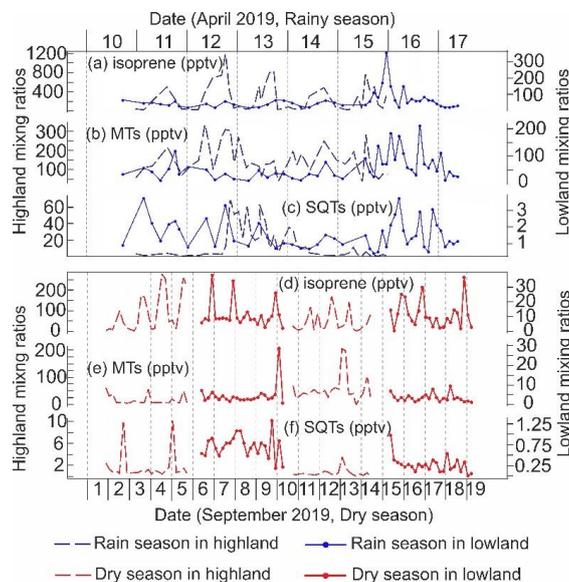
Figure 4. Biogenic volatile organic compound mixing ratios in the highland and lowland ecosystems during the rainy and dry seasons: **(a, d)** isoprene, **(b, e)** monoterpenoids (MTs), **(c, f)** sesquiterpenes (SQTs).

The mixing ratio of isoprene showed distinct diurnal variation in the highlands during both the rainy and dry seasons, but in the lowlands only during the dry season. The mixing ratio of isoprene increased in the morning, coinciding with sunrise, and stayed high during the rest of the day. The measured mixing ratio of isoprene contributed on average 37 % and 84 % in the highlands and lowlands, respectively, to the total BVOC mixing ratio (Fig. 5).

The mixing ratios of MTs showed an opposite daily pattern than that of isoprene, with higher mixing ratios during
255 nighttime. MTs with a higher mixing ratio during nighttime than daytime have been observed in earlier studies of MTs
in savannas in South Africa (Gierens et al., 2014), and needleleaf forest in California, and Finland (Bouvier-Bown et al.,
2009; Hakola et al., 2012). Even though the MT emissions are expected to be highest during daytime, the mixing ratio of
MTs is lower since the mixing, and therefore dilution, is highest during daytime and lowest during the night (Mogensen
et al., 2011; Hellén et al., 2018).

260 The diurnal maximum mixing ratio of MTs was on average 254 and 89 pptv in the rainy season, and 56 and 11.5 pptv
in the dry season, in the highlands and lowlands, respectively, and MTs thus dominated the total BVOC mixing ratio
during nighttime (Fig. 5). The diurnal variations of α-pinene and limonene controlled the changes in total MT mixing
ratio and contributed over 60 % to the total MT mixing ratio. Decreasing mixing ratios of limonene between day and
night led the diurnal variation of the total mixing ratio of MTs in the rainy season, while decreasing α-pinene controlled
265 the diurnal variation of total MTs in the dry season. The minimum diurnal mixing ratio of MTs occurred in the early night
during the rainy season and around noon in the dry season.
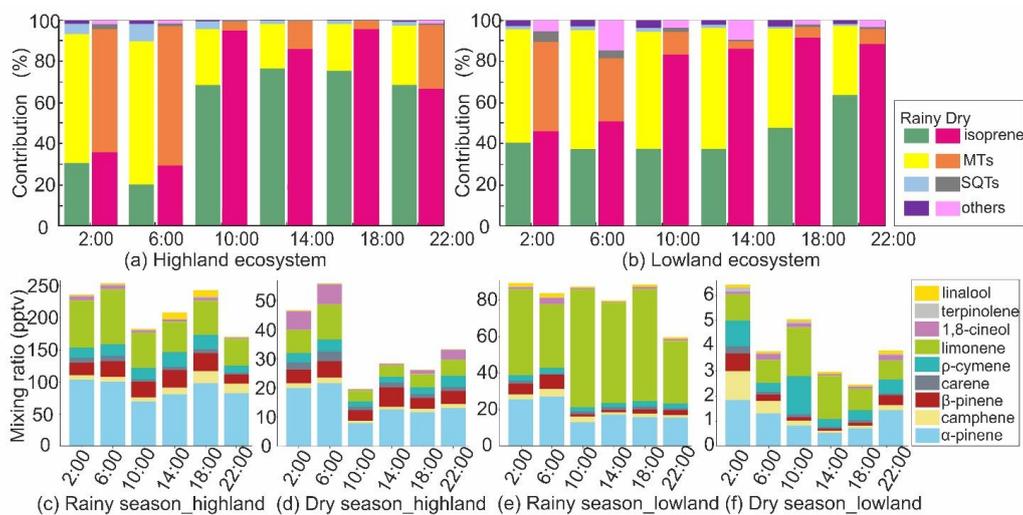
Figure 5. Diurnal contribution of biogenic volatile organic compounds **(a, b)** and mixing ratio of monoterpenoids
(MTs) **(c, d, e, f)** across the highland site and the lowland site in the rainy and the dry seasons. SQTs = sesquiterpenes,
270 others = 2-methyl-3-buten-2-ol and bornyl acetate.

The isoprene mixing ratio ranged from 730 to 1820 pptv in the rainy season of 1996 in a tropical forest in northern
Congo, which was covered by evergreen or semi-evergreen trees (Serça et al., 2001). A similar level of isoprene mixing
ratio was observed in a forest ecosystem near Enyela, northern Congo, with values ranging from 700 to 1000 pptv at the
end of the rainy season of 1996 (Greenberg et al., 1999). In western Africa, isoprene mixing ratios of over 1000 pptv
275 during daylight hours were measured in a forest surrounded by a woodland savanna ecosystem in Benin (Saxton et al.,
2007). The western Africa and the two central Africa measurements aforementioned all showed at least an order of
magnitude higher isoprene mixing ratios compared with the measurements in the highlands (Wundanyi) of this study
(Table 1). The measured mixing ratios of α-pinene, limonene, and β-pinene in Wundanyi were comparable to the
corresponding compound levels from the aforementioned forest measurements. The mixing ratios of isoprene and MTs
280 in Wundanyi are comparable to our previous measurements from three types of montane native forests of Taita Hills in

southern Kenya (Liu et al., 2021). The mixing ratios of isoprene and MTs at the lowland site in Maktau were about four times lower than the corresponding levels measured from savanna ecosystems in Central Africa Republic (Boali) and South Africa (Greenberg et al., 1999; Harley et al., 2003), and grass, shrubland in western Senegal (Grant et al., 2008), and considerably lower than the corresponding compound levels from woodland in Botswana (Greenberg et al., 2003).

285 The mixing ratios of isoprene and limonene in the rainy season in Maktau are higher than the levels of the corresponding compounds in grassland in Welgegund, South Africa, while the mixing ratios of α-pinene and β-pinene, both in the rainy and the dry seasons, as well as isoprene and limonene in the dry season in Maktau, were lower than the values reported by Jaars et al. (2016). The mixing ratios of α-pinene, limonene, and β-pinene in the rainy season in Maktau were all in the range of the mixing ratios of the corresponding compounds in our previous measurements, while that of isoprene was

290 at lower levels than previously reported (Liu et al., 2021).

Table 1. Mixing ratios of biogenic volatile organic compound in different ecosystems in Africa (mixing ratios are presented as mean values, except those with extra explanations, e.g., "midday," "minimum/maximum").

Location	Time	Vegetation	Compound	Mixing ratio (pptv)	Reference
Wundanyi, Kenya (38.4° E, 3.4° S)	April and September 2019	Agroforestry	Isoprene	Rainy: 69 to 809 Dry: 17 to 156	This study
			α-Pinene	Rainy: 70 to 103 Dry: 8 to 22	
			Limonene	Rainy: 42 to 86 Dry: 4 to 12	
			β-Pinene	Rainy: 14 to 28 Dry: 4 to 7	
Maktau, Kenya (32.7° E, 3.3° S)		Savanna bushland	Isoprene	Rainy: 52 to 115 Dry: 8 to 25	
			α-Pinene	Rainy: 13 to 27 Dry: 0.5 to 1.8	
			Limonene	Rainy: 34 to 64 Dry: 0.8 to 1.9	
			β-Pinene	Rainy: 1 to 8 Dry: 0.1 to 0.7	
Enyele, Democratic Republic of the Congo (18° E, 3° N)	November and December 1996	Forest	Isoprene	700 to 1000	Greenberg et al., 1999
			α-Pinene	30 to 100	
Boali, Central African Republic (18° E, 4.5° N)		Savanna	Isoprene	100 to 400	
			α-Pinene	20 to 30	
Northern Congo (16.2° E, 2.1° S)	March 1996	Tropical evergreen	Isoprene	1820 ± 870	Serça et al., 2001
	November 1996		Isoprene	730 ± 480	

Location	Date	Vegetation	Compound	Mixing ratio	Reference
	March and November 1996	forest, semi-evergreen forest	β-Pinene	< 10	
South Africa (29.8° E, 25.0° S)	February 2001	*Combretum–Acacia* savanna	Isoprene	Midday 390	Harley et al., 2003
Botswana (23.3° E, 19.5° S)	February 2001	Mopane woodland	α-Pinene	Minimum < 1000 Maximum > 2000	Greenberg et al., 2003
Benin (1.4° E, 9.4° N)	June 2006	Forest	Isoprene	Day_maximum > 1000 Night_maximum > 500	Saxton et al., 2007
			Limonene	Few tens to 5000	
Republic of Senegal (17.1° W 14.7° N)	September 2006	Grasses, shrubs	Isoprene	Minimum 200 Maximum 400	Grant et al., 2008
Benin (2.7° E, 10.1° N)	August 17, 2006	Subtropical forest	Isoprene	Midday 1184 294 ± 333	Stone et al., 2010
Welgegund, South Africa (26.9° E, 26.6° S)	February 2011 to February 2012; & December 2013 to February 2015	Grassland	Isoprene	23 to 28	Jaars et al., 2016
			α-Pinene	57 to 71	
			Limonene	30 to 54	
			β-Pinene	5 to 19	
Kenya (32 to 38° E, 3.2 to 3.4° S)	April 2019	Montane forest	Isoprene	564 to 812	Liu et al., 2021
			α-Pinene	28 to 175	
			Limonene	3 to 23	
			β-Pinene	4 to 17	
		Grass and shrubs	Isoprene	614 to 768	
			α-Pinene	10 to 28	
			Limonene	11 to 196	
			β-Pinene	1.8 to 4.4	

3.1.2 Mixing ratios of sesquiterpenes, MBO, and bornyl acetate

The mixing ratios of SQTs were low and contributed to around 3 % of the total BVOC mixing ratios in all samples. SQTs
295 showed seasonal and diurnal variations similar to those of MTs, but their mixing ratio was much lower than that of MTs,
with seasonal mean SQT mixing ratios of 15.0 ± 19 pptv and 1.5 ± 0.9 pptv in the rainy season, and 1.1 ± 2 pptv and 0.5
± 0.3 pptv in the dry season, in the highlands and lowlands, respectively. SQTs are very reactive and therefore their
contribution to the local atmospheric chemistry can still be significant. The highest daily means were measured during
the nighttime, which was the same as in the case of the MTs. β-caryophyllene showed the highest mixing ratios among

300 the SQTs, followed by β-farnesene and/or α-humulene measured in both the rainy and dry seasons. The diurnal trend of β-caryophyllene and β-farnesene followed the variation of total SQTs.

  The mixing ratios of MBO and bornyl acetate were both low. MBO explained 2.6 % of the total BVOC mixing ratio of all samples, while bornyl acetate explained 0.5 %. Both compounds have seasonal and diurnal variations. The seasonal mean mixing ratios of MBO and bornyl acetate were 5 and 1.5 times higher in the rainy season than in the dry season in

305 the highlands, respectively, and the mixing ratios of both BVOCs were 6 times higher in the lowlands. The diurnal mean mixing ratios of MBO and bornyl acetate were around 4 and 0.8 pptv in the rainy season in both the highlands and lowlands. MBO mixing ratios were 1 and 0.7 pptv in the dry season in the highlands and lowlands, while that of bornyl acetate was 0.6 and 0.1 pptv, respectively. The daily mean mixing ratio of bornyl acetate was lower than 1 pptv in the rainy and dry seasons both in the highlands and lowlands.

310 Jaars et al. (2016) measured MBO for the first time in Africa, and they reported that the mean mixing ratios of MBO were 12 pptv and 8 pptv in their first and second campaign, respectively, which are higher than the mean MBO mixing ratios measured in the highlands and lowlands in this study. Guenther (2013) stated that MBO is emitted from most isoprene–emitting vegetation at an emission rate of ∼ 1 % of that of isoprene. The Welgegund data (Jaars et al., 2016) showed that MBO is approximately 30 % of the isoprene mixing ratio, and thus their study indicated that MBO at

315 Welgegund is most likely from other MBO emitting species than from isoprene emitters. MBO are higher than 1 % of isoprene mixing ratios in our study, which was 3.7 % and 6.3 % of the isoprene mixing ratio in the highlands in the rainy and dry seasons, respectively, and 7.6 % and 9.8 % in the lowlands. Unfortunately, we could not partition the source of MBO emitter(s) in this study area during our measurements.

3.2 Reactivity of the measured BVOCs with oxidants

320 The reactivity toward O_3, OH, and NO_3 was calculated using the measured BVOC mixing ratios (Fig. 6). The O_3 reactivity of SQTs was 5 to 30 times higher than for other BVOCs, with β-caryophyllene having the highest contribution to the total O_3 reactivity. The strong relative importance of the SQTs compared with other BVOCs for the local O_3 reactivity has also been seen in the ambient air of a Scots pine forest in Finland (Hellén et al., 2018). Out of the total BVOCs, MTs contributed most to the NO_3 reactivity, an average of 13 and 15 times more than isoprene and SQTs, respectively. MTs

325 also contributed to the OH reactivity, with a 0.7 to 1.9 times higher contribution than isoprene during nighttime, while isoprene is the dominant BVOC contributor to the OH reactivity during the day, with 3.1 to 3.5 times higher contributions than MTs.

  Isoprene shows the highest mixing ratio of BVOCs in this study. The atmospheric lifetime of isoprene is 34 hours and 2.3 hours with O_3 and OH, respectively. Follow that of isoprene, limonene (∼ 2 hours) and α-pinene (∼ 4 hours) have

330 higher mixing ratios, and are detected to have a relatively short lifetime with OH and O_3 compared with other MTs (except terpinolene and linalool). Higher importance of limonene and α-pinene for OH reactivity than other MTs was also observed in a savanna ecosystem in South Africa (Jaars et al., 2016), which reported that both compounds also had higher mixing ratios than other MTs during their campaigns. Compared with other MTs, limonene has a significantly higher yield for highly oxygenated organic molecules (Ehn et al., 2014; Bianchi et al., 2019), which has been found to be a major

335 component of secondary organic aerosols (e.g., Ehn et al., 2014; Mutzel et al., 2015), for which higher limonene is expected to have a strong impact on local aerosol production in southern Kenya as well. The low mixing ratios of β-caryophyllene and α-humulene have shorter lifetimes with OH and O_3 than other SQTs and BVOCs. The lifetimes of β-caryophyllene and α-humulene are a few minutes with O_3 and about 1 hour with OH (Table A3).
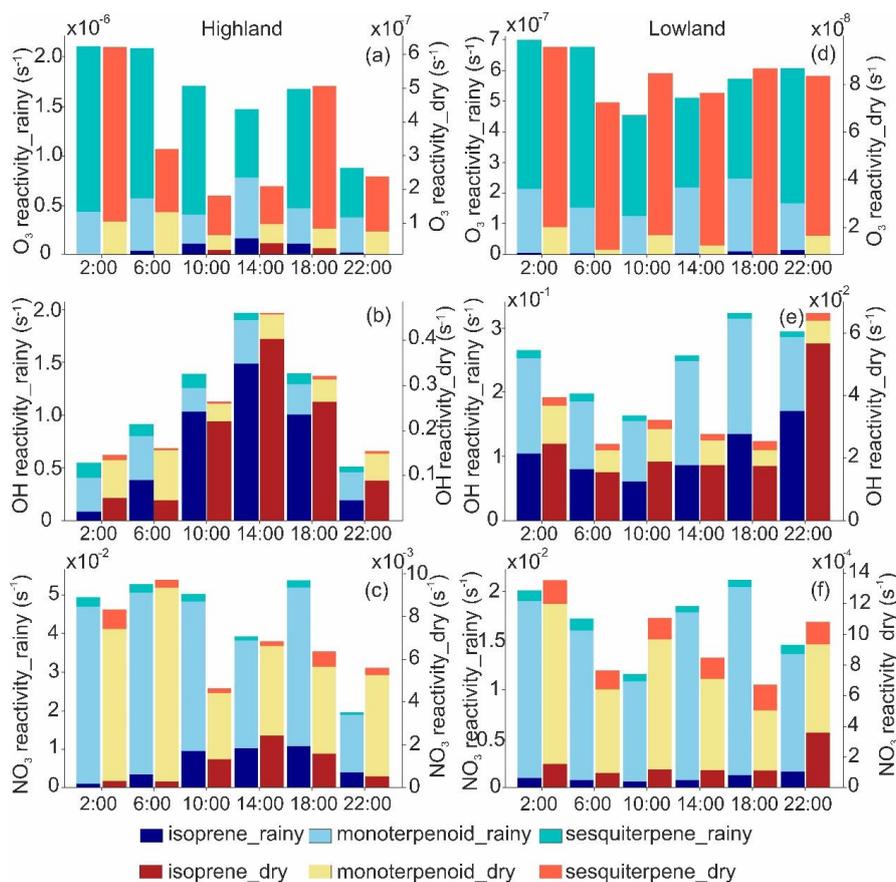
340 **Figure 6.** Reactivity of ozone (O_3), hydroxyl (OH), and nitrate (NO_3) of different biogenic volatile organic compounds in the highland **(a, b, c)** and lowland ecosystems **(d, e, f)** in the rainy and dry seasons.

3.3 Estimation of BVOC emission factors

The EFs for isoprene, MBO, and detected MTs, for the agriculture savanna ecosystem surrounding the Maktau site, were estimated for the rainy and dry seasons separately (Fig. 7). The median values of the EF for α-pinene, β-pinene, 3Δ-

345 carene, camphene, and limonene (Fig. 7c to g) are higher during the rainy season in April than during the dry season in September, while the median values of the EF for MBO (Fig. 7b) and all other MTs (Fig. 7g) are higher during the dry season than during the rainy season. If the dependency of soil moisture availability on the emission of isoprene is considered, then the EF for isoprene during both the rainy and dry seasons is effectively the same (Fig. 7a). Considering the variability in the estimated EFs for the two different seasons, only the EFs for limonene show no overlap in the

350 indicated error bars (Fig. 7f), which are defined by the minimum and maximum daily estimated EF. Thus, our results suggest that the EF for limonene might be seasonally dependent.

In order to put the estimated EFs into context and to contribute to an improved representation of BVOC emissions from African ecosystems in models, the estimated EFs are compared with the EFs used in MEGAN v2.1 for warm C4 grass and Crop1 (Guenther et al., 2012). The estimated EFs for isoprene (155 µg m^{-2} h^{-1} in the rainy season,

355 280 µg m^{-2} h^{-1} in the dry season) and β-pinene (2 µg m^{-2} h^{-1} in the rainy season, 1.5 µg m^{-2} h^{-1} in the dry season)

compare very well with the EFs used in MEGAN for warm C4 grass (Fig. 7a, d), and in the case of β-pinene, also for Crop1, since MEGAN assumes the same EF for β-pinene for the two different plant functional types. The estimated median EFs for MBO, α-pinene, 3Δ-carene, and limonene are higher than the EFs used in MEGANv2.1 by about 8 (4), 17 (53), 1 (2), and 89 (314) $\mu g\ m^{-2}\ h^{-1}$, respectively, where the values in parenthesis are for the rainy season, while the

360 others are for the dry season. The values of the estimated EFs compare best with the EFs allocated for warm C4 grass in MEGAN in the case of isoprene, α-pinene, β-pinene, and 3Δ-carene compared with the EFs for other plant functional types in MEGAN. However, the estimated EF for limonene is more in line with MEGAN's EF for tropical trees (80 $\mu g\ m^{-2}\ h^{-1}$). Unfortunately, we could not identify the source of the limonene emitter(s). It could be the native African shrubs surrounding the lowland site, which are dominated by acacias (*Vachellia mellifera, VachelliaAcacia tortilis*), but

365 to our knowledge emission rates have not been reported from these species. The estimated EF for MBO is much higher than that used for C4 grass in MEGAN. The EF for the sum of other MTs (i.e., six MTs at our site and up to 34 in MEGAN) is about 10 and 20 $\mu g\ m^{-2}\ h^{-1}$ higher than that assumed in MEGAN for warm C4 grass and Crop1 for the rainy and dry seasons, respectively (Fig. 7g). During both seasons, linalool contributes the most to the total EF for the sum of other MTs in this study, while terpinolene accounts for the second largest fraction.

370
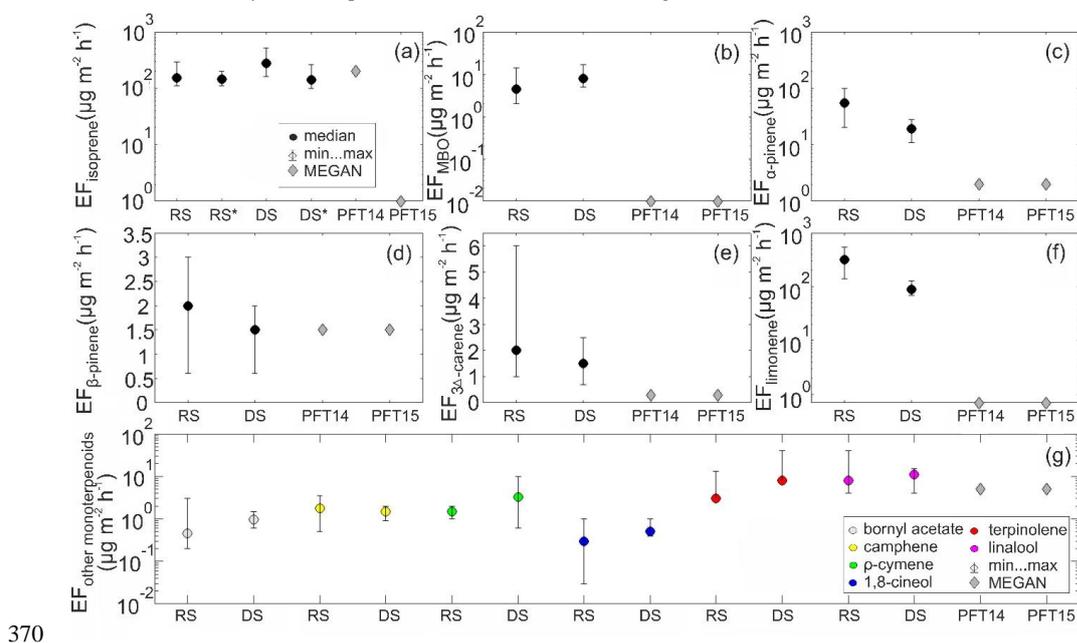
Figure 7. Estimated biogenic volatile organic compound (BVOC) emission factors (EF) for the agriculture savanna ecosystem surrounding the Maktau field site in comparison with the EFs for warm C4 grass (PFT14) and Crop1 (PFT15) used in MEGAN v2.1. The EFs have been estimated for the rainy season (RS, April) and for the dry season (DS, September) separately. **(a)** isoprene (The EF was estimated by either considering (RS, DS) or neglecting (RS*, DS*) a

375 dependency of the activity factor on soil moisture availability), **(b)** 2-methyl-3-buten-2-ol, **(c)** α-pinene, **(d)** β-pinene, **(e)** 3Δ-carene, **(f)** limonene, and **(g)** other monoterpenes, which includes the sum of up to 34 other monoterpenes in MEGANv2.1 and includes bornyl acetate (gray), camphene (yellow), ρ-cymene (green), 1,8-cineol (blue), terpinolene (red), and linalool (magenta) at Maktau Weather Station. The legend provided in **(a)** is valid for **(a)** to **(f)**.

We emphasize that the estimated EFs are connected with a large degree of uncertainty, since they are not based on
380 flux measurements from the site but are instead determined using observed BVOC mixing ratios and an inverse modeling
approach, which is limited by model assumptions and inputs.

4 Conclusion

In this study we measured mixing ratios of isoprene, MTs, SQTs, bornyl acetate, and MBO in the humid highland and
dry lowland ecosystems in Taita Taveta County, southern Kenya, during both a rainy and a dry season.

385 Isoprene and MTs showed the highest mixing ratios in both the highlands and lowlands, while α-pinene, limonene,
and β-pinene accounted for the largest contribution to the total mixing ratio of MTs. Isoprene dominated the total BVOC
mixing ratio during daytime and reached diurnal peak mixing ratios in the afternoon in the highlands and in the early
evening in the lowlands. The mixing ratio of MTs generally peaked between midnight and early morning, and MTs
dominated the total BVOC mixing ratio during nighttime. Isoprene was the dominant BVOC contributor to the OH
390 reactivity, MTs dominated the NO_3 reactivity of BVOCs, and SQTs showed higher contributions to the O_3 reactivity of
BVOCs than isoprene and MTs.

Using an inverse model approach with measured BVOC mixing ratios and meteorology data, we estimated the EFs
for isoprene, MBO, and MTs in the agriculture savanna ecosystem. The estimated EFs for isoprene and β-pinene agreed
very well with what is currently assumed in MEGANv2.1, for warm C4 grass, but the estimated EFs for MBO, α-pinene,
395 and especially limonene were significantly higher than what is assumed in MEGAN for the relevant plant functional type.
Additionally, our results indicate that the EF for limonene might be seasonally dependent.

Appendix A:

Table A1. Sample and flow rate measurements in Taita and Maktau field site during the rainy and dry season (sccm: standard cubic centimeters per minute).

	Wundanyi Station (humid highland)		Maktau field site (dry lowland)	
	first campaign	second campaign	first campaign	second campaign
rainy season (2019)	Apr 10th to 13th 4 h/tube 100.5 sccm	Apr 13th to 15th 2 h/tube 99.5 sccm	Apr 10th to 13th 4 h/tube 70 sccm	Apr 14th to 17th 2 h/tube 67 sccm
dry season (2019)	Sept 1st to 5th 4h/tube 85.5 sccm	Sept 10th to 14th 4h/tube 81.5 sccm	Sept 6th to 10th 4h/tube 83 sccm	Sept 16th to 19th 4h/tube 92 sccm

Table A2. Reaction rate coefficients ($k_{i,x}$) applied in the model used for estimations of the emission factors and for reactivity calculations. T (K) is air temperature.

Compound	k_{O3} (cm³ s⁻¹)	Reference	k_{OH} (cm³ s⁻¹)	Reference
Isoprene	$1.03 \cdot 10^{-14}$ $\cdot e\left(\frac{-1995}{T}\right)$	IUPAC preferred value (http://iupac.pole-ether.fr/htdocs/datasheets/xhtml/Ox_VOC7_O3_CH2C(CH3)CHCH2.xhtml_mathml.xml)	$2.70 \cdot 10^{-11}$ $\cdot e\left(\frac{390}{T}\right)$	Master Chemical Mechanism, MCM v3.2 (Jenkin et al., 1997; Saunders et al., 2003), via website: http://mcm.leeds.ac.uk/MCM
MBO	$1.0 \cdot 10^{-17}$	Grosjean and Grosjean (1994)	$8.1 \cdot 10^{-12}$ $\cdot e\left(\frac{610}{T}\right)$	Rudich et al. (1995)
Bornyl acetate	-	bornyl acetate does not react with O₃, because it is a saturated hydrocarbon	$13.9 \cdot 10^{-12}$	Coeur et al. (1999)
α-Pinene	$8.05 \cdot 10^{-16}$ $\cdot e\left(\frac{-640}{T}\right)$	IUPAC preferred value (http://iupac.pole-ether.fr/htdocs/datasheets/pdf/Ox_VOC8_O3_apinene.pdf)	$1.2 \cdot 10^{-11}$ $\cdot e\left(\frac{440}{T}\right)$	IUPAC preferred value (http://iupac.pole-ether.fr/htdocs/datasheets/xhtml/HOx_VOC9_HO_apinene.xhtml_mathml.xml)
Camphene	$9.0 \cdot 10^{-19}$	Atkinson (1997)	$5.3 \cdot 10^{-11}$	Atkinson (1997)
β-Pinene	$1.35 \cdot 10^{-15}$ $\cdot e\left(\frac{-1270}{T}\right)$	IUPAC preferred value (http://iupac.pole-ether.fr/htdocs/datasheets/pdf/Ox_VOC19_O3_bpinene.pdf)	$2.38 \cdot 10^{-11}$ $\cdot e\left(\frac{357}{T}\right)$	Kleindienst et al. (1982)
3Δ-Carene	$3.7 \cdot 10^{-17}$	Atkinson (1997)	$8.8 \cdot 10^{-11}$	Atkinson (1997)
ρ-Cymene	$5.0 \cdot 10^{-20}$	Hellén et al. (2018)	$1.5 \cdot 10^{-11}$	Corchnoy and Atkinson (1990)
Limonene	$2.80 \cdot 10^{-15}$ $\cdot e\left(\frac{-770}{T}\right)$	IUPAC preferred value (http://iupac.pole-ether.fr/htdocs/datasheets/pdf/Ox_VOC20_O3_limonene.pdf)	$4.28 \cdot 10^{-11}$ $\cdot e\left(\frac{401}{T}\right)$	Gill and Hites (2002)
1,8-Cineol	$1.5 \cdot 10^{-19}$	Hellén et al. (2018)	$1.11 \cdot 10^{-11}$	Corchnoy and Atkinson (1990)
Terpinolene	$1.88 \cdot 10^{-15}$	Shu and Atkinson (1994)	$22.5 \cdot 10^{-11}$	Corchnoy and Atkinson (1990)
Linalool	$4.3 \cdot 10^{-16}$	Atkinson et al. (1995)	$15.9 \cdot 10^{-11}$	Atkinson et al. (1995)

405

Table A3. Data variation and O_3, OH and NO_3 reaction rate coefficients ($k_{i,x}$, values were shown in daily average) for various BVOCs (RSD: relative standard deviation, unit in %; k unit in cm^3s^{-1}; τ unit in hour)

Compound	Season	RSD	k_O_3	k_OH	k_NO_3	τ_O_3	τ_OH
Isoprene	Maktau_rainy	101.19	1.26E-17	1.00E-10	6.50E-13	32.6	2.2
	Maktau_dry	80.34	1.18E-17	1.02E-10	6.39E-13	33.5	2.4
	Taita_rainy	112.83	1.15E-17	1.02E-10	6.37E-13	31.9	2.2
	Taita_dry	112.24	1.07E-17	1.04E-10	6.26E-13	37.1	2.4
α-Pinene	Maktau_rainy	96.35	9.36E-17	5.27E-11	6.23E-12	4.4	4.2
	Maktau_dry	117.30	9.15E-17	5.35E-11	6.35E-12	4.3	4.6
	Taita_rainy	48.39	9.09E-17	5.38E-11	6.38E-12	4.0	4.1
	Taita_dry	124.54	8.88E-17	5.46E-11	6.49E-12	4.5	4.5
Camphene	Maktau_rainy	111.89	9.0E-19	5.3E-11	6.6E-13	458.6.9	4.2
	Maktau_dry	272.87	9.0E-19	5.3E-11	6.6E-13	437.9	
	Taita_rainy	194.68	9.0E-19	5.3E-11	6.6E-13	408.6	
	Taita_dry	90.17	9.0E-19	5.3E-11	6.6E-13	440.8	
β-Pinene	Maktau_rainy	146.87	1.89E-16	7.90.E-10	2.5E-12	21.8	2.8
	Maktau_dry	189.67	1.81E-17	8.01E-11	2.5E-12	21.8	3.1
	Taita_rainy	74.68	1.78E-17	8.04E-11	2.5E-12	20.6	2.8
	Taita_dry	102.85	1.70E-17	8.14E-11	2.5E-12	23.3	3.0
Limonene	Maktau_rainy	93.67	2.10E-17	1.65E-11	1.2E-11	2.0	1.3
	Maktau_dry	67.97	2.05E-16	1.67E-10	1.2E-11	1.9	1.5
	Taita_rainy	53.66	2.03E-16	1.68E-10	1.2E-11	1.8	1.3
	Taita_dry	142.89	1.97E-16	1.70E-10	1.2E-11	2.0	1.4
ρ-Cymene*	Maktau_rainy	74.49	5.00E-20	1.11E-11		8254.9	14.7
	Maktau_dry	156.80	5.00E-20	1.11E-11		7882.7	16.2
	Taita_rainy	107.31	5.00E-20	1.11E-11		7354.1	14.7
	Taita_dry	96.52	5.00E-20	1.11E-11		7934.0	16.2
3Δ-Carene	Maktau_rainy	129.99	3.7E-17	2.25E-11	9.1E-12	11.2	2.5
	Maktau_dry	146.98	3.7E-17	2.25E-11	9.1E-12	10.7	2.8
	Taita_rainy	79.57	3.7E-17	2.25E-11	9.1E-12	9.9	2.5
	Taita_dry	107.19	3.7E-17	2.25E-11	9.1E-12	10.7	2.8
18-Cineol	Maktau_rainy	195.09	1.5E-19	1.59E-11		2751.6	20.0

	Maktau_dry	88.31	1.5E-19	1.59E-11		2627.6	22.1
	Taita_rainy	107.14	1.5E-19	1.59E-11		2451.4	20.0
	Taita_dry	214.96	1.5E-19	1.59E-11		2644.7	22.1
Terpinolene	Maktau_rainy	141.35	1.88E-15	2.25E-10	9.7E-11	0.2	1.0
	Maktau_dry	284.61	1.88E-15	2.25E-10	9.7E-11	0.2	1.1
	Taita_rainy	84.71	1.88E-15	2.25E-10	9.7E-11	0.2	1.0
	Taita_dry	133.40	1.88E-15	2.25E-10	9.7E-11	0.2	1.1
Linalool	Maktau_rainy	141.69	4.3E-16	1.59E-10	1.10E-11	1.0	1.4
	Maktau_dry	73.08	4.3E-16	1.59E-10	1.10E-11	0.9	1.5
	Taita_rainy	467.26	4.3E-16	1.59E-10	1.10E-11	0.9	1.4
	Taita_dry	120.62	4.3E-16	1.59E-10	1.10E-11	0.9	1.5
Longicyclene	Maktau_rainy	96.75	5.0E-19	4.7E-11	6.8E-13	825.5	4.7
	Maktau_dry	618.05	5.0E-19	4.7E-11	6.8E-13	788.3	5.2
	Taita_rainy	110.58	5.0E-19	4.7E-11	6.8E-13	735.4	4.7
	Taita_dry	133.07	5.0E-19	4.7E-11	6.8E-13	793.4	5.2
Iso-longifolene	Maktau_rainy	326.40	1.0E-17		3.9E-12	41.3	
	Maktau_dry	618.05	1.0E-17		3.9E-12	39.4	
	Taita_rainy	366.74	1.0E-17		3.9E-12	36.8	
	Taita_dry	685.57	1.0E-17		3.9E-12	39.7	
β-Caryophyllene	Maktau_rainy	89.74	1.2E-14	2.0E-10	1.9E-11	0.0	1.1
	Maktau_dry	93.96	1.2E-14	2.0E-10	1.9E-11	0.0	1.2
	Taita_rainy	100.02	1.2E-14	2.0E-10	1.9E-11	0.0	1.1
	Taita_dry	276.94	1.2E-14	2.0E-10	1.9E-11	0.0	1.2
β-Farnesene	Maktau_rainy	134.45	5.59E-16	2.3E-10	1.9E-11	0.7	1.0
	Maktau_dry	76.79	5.59E-16	2.3E-10		0.7	1.1
	Taita_rainy	144.76	5.59E-16	2.3E-10		0.7	1.0
	Taita_dry	113.73	5.59E-16	2.3E-10		0.7	1.1
α-Humulene	Maktau_rainy	61.93	1.2E-14	2.9E-10	3.5E-11	0.0	0.8
	Maktau_dry	60.92	1.2E-14	2.9E-10	3.5E-11	0.0	0.8
	Taita_rainy	78.56	1.2E-14	2.9E-10	3.5E-11	0.0	0.8
	Taita_dry	87.74	1.2E-14	2.9E-10	3.5E-11	0.0	0.8
MBO	Maktau_rainy	69.37	1.0E-17	6.30E-11	1.20E-14	41.3	3.5

	Maktau_dry	68.78	1.0E-17	6.44E-11	1.20E-14	39.4	3.8
	Taita_rainy	92.89	1.0E-17	6.48E-11	1.20E-14	36.8	3.4
	Taita_dry	109.41	1.0E-17	6.63E-11	1.20E-14	39.7	3.7
Bornyl acetate	Maktau_rainy	174.73		1.39E-11			16.0
	Maktau_dry	77.48		1.39E-11			17.6
	Taita_rainy	78.44		1.39E-11			16.0
	Taita_dry	77.05		1.39E-11			17.6

Calculation methods of k values were shown in Table A2.

Data availability. BVOC mixing ratios and meteorological data used in this work are available from the authors upon
410 request *(yang.z.liu@helsinki.fi and petri.pellikka@helsinki.fi).*

Author contributions. Y.L., S.S., H.H., and P.P. planned the measurement protocol and Y.L., S.S., L.M., and P.P.
performed the measurements in Kenya, while T.T. conducted the laboratory analysis in Finland. Y.L., T.T., and H.H.
performed the data interpretation and analysis. M.R. calculated MLHs. D.T. developed the BVOC emissions and
chemistry model for estimating BVOC EFs, conducted the simulations, and wrote the sections related to this work. Y.L.
415 wrote the paper with contributions from all authors. The final version of the manuscript was approved by all authors.

Competing interests. The authors declare that they have no conflict of interest.

Acknowledgements. This work was supported by the University of Helsinki and its Taita Research Station, the Finnish
Meteorology Institute, the Mazingira Centre of the International Livestock Research Institute, the China Scholarship
Council fellowship (funding no. 201806040217), Academy of Finland projects (nos 318645, 316151, 323255, 307957,
420 and 275608), and Academy of Finland Flagship funding (grant no. 337552). Research permit P/18/97336/26355 from the
National Council for Science and Technology of Kenya is greatly acknowledged. We appreciate Ms. Cathryn Primrose-
Mathisen for language editing, the staff of the Taita Research Station of the University of Helsinki for the logistics and
Mr. Mjomba Mwadime for his help with sample collection.

References

425 Aalto, J., Kolari, P., Hari, P., Kerminen, V. M., Schiestl, Aalto, P., Aaltonen, H., Levula, J., Siivola, E., Kulmala, M., and
Bäck, J.: New foliage growth is a significant, unaccounted source for volatiles in boreal evergreen forests,
Biogeosciences, 11, 1331–1344, https://doi.org/10.5194/bg-11-1331-2014, 2014.

Amara, E., Adhikari, H., Heiskanen, J., Siljander, M., Munyao, M., Omondi, P., and Pellikka, P.: Aboveground biomass
distribution in a multi-use savannah landscape in southeastern Kenya: impact of land use and fences. Land 2020, 9,
430 381, https://doi.org/10.3390/land9100381, 2020.

Andersson, S., Nilsson, L.A., Groth, I., and Bergstrom, G.: Floral scents in butterfly-pollinated plants: possible
convergence in chemical composition. Botanical Journal of the Linnean Society, 140, 129–153,
https://doi.org/10.1046/j.1095-8339.2002.00068.x, 2002.

Atkinson, R: Gas-phase tropospheric chemistry of Volatile Organic Compounds: 1. Alkanes and alkenes, J. Phys. Chem.
435   Ref. Data, 26, 215-290, doi: 10.1063/1.556012, 1997.

Atkinson, R., Arey, J., Aschmann, S. M., Corchnoy, S. B., and Shu, Y.: Rate constants for the gas-phase reactions of *cis*-3-Hexen-1-ol, *cis*-3-Hexenylacetate, *trans*-2-Hexenal, and Linalool with OH and NO3 radicals and O3 at 296 ± 2 K, and OH radical formation yields from the O3 reactions, Int. J. Chem. Kinet., 27, 941-955, https://doi.org/10.1002/kin.550271002, 1995.

440 Ayugi, B.O., Wang, W., and Chepkemoi, D.: Analysis of spatial and temporal patterns of rainfall variations over Kenya. Environ Earth Sci, 6, 69–83, 2016.

Bianchi, F., Kurtén, T., Riva, M., Mohr, C., Rissanen, M. P., Roldin, P., Berndt, T., Crounse, J. D., Wennberg, P. O., Mentel, T. F., Wildt, J., Junninen, H., Jokinen, T., Kulmala, M., Worsnop, D. R., Thronton, J. A., Donahue, N., Kjaergaard, H. G., and Ehn, M.: Highly oxygenated organic molecules (HOM) from gas-phase autoxidation
445   involving peroxy radicals: A key contributor to atmospheric aerosol, Chem. Rev., 119, 3472–3509, https://doi.org/10.1021/acs.chemrev.8b00395, 2019.

Bonn, B., Magh, R. K., Rombach, J., and Kreuzwieser, J.: Biogenic isoprenoid emissions under drought stress: different responses for isoprene and terpenes, Biogeosciences, 16, 4627–4645, https://doi.org/10.5194/bg-16-4627-2019, 2019.

Bouvier-Brown, N. C., Goldstein, A. H., Gilman, J. B., Kuster, W. C., and de Gouw, J. A.: In-situ ambient quantification
450   of monoterpenes, sesquiterpenes, and related oxygenated compounds during BEARPEX 2007: implications for gas- and particle-phase chemistry, Atmos. Chem. Phys., 9, 5505–5518, https://doi.org/10.5194/acp-9-5505-2009, 2009.

Campbell, G. S., and Norman, J. M.: An Introduction to Environmental Biophysics, Springer, New York, 1998.

Claeys, M., Graham, B., Vas, G., Wang, W., Vermeylen, R., Pashynska, V., Cafmeyer, J., Guyon, P., Andreae, M. O., Artaxo, P., Maenhaut W.: Formation of secondary organic aerosols through photooxidation of isoprene, Science, 303,
455   1173–1176, doi: 10.1126/science.1092805, 2004.

Coeur, C., Jacob, V., and Foster, P.: Gas phase reaction of hydroxyl radical with the natural hydrocarbon bornyl acetate, Phys. Chem. Earth C: Sol. Terr. Planet. Sci., 24, 537-539, https://doi.org/10.1016/S1464-1917(99)00087-2, 1999.

Combe, M., Vilà-Guerau de Arellano, J., Ouwersloot, H. G., Jacobs, C. M. J., and Peters, W.: Two perspectives on the coupled carbon, water and energy exchange in the planetary boundary layer, Biogeosciences, 12, 103–123,
460   https://doi.org/10.5194/bg-12-103-2015, 2015.

Corchnoy, S. B., and Atkinson, R.: Kinetics of the gas-phase reaction of hydroxyl and nitrogen oxide (NO3) radicals with 2-carene, 1,8-cineole, p-cymene, and terpinolene, Environ. Sci. Technol., 24, 1497-1502, https://doi.org/10.1021/es00080a007, 1990.

Ehn, M., Thornton, J. A., Kleist, E., Sipilä, M., Junninen, H., Pullinen, I., Springer, M., Rubach, F., Tillmann, R., Lee,
465   B., Lopez-Hilfiker, F., Andres, S., Acir, I-H., Rissanen, M., Jokinen, T., Schobesberger, S., Kangasluoma, J., Kontkanen, J., Nieminen, T., Kurtén, T., Nielsen, L. B., Jørgensen, S., Kjaergaard, H. G., Canagaratna, M., Maso, M. D., Berndt, T., Petäjä, T., Wahner, A., Kerminen, V.-M., Kulmala, M., Worsnop, D. R., Wildt, J., and Mentel, T. F.: A large source of low-volatility secondary organic aerosol, Nature 506, 476–479, https://doi.org/10.1038/nature13032, 2014.

470 Emmerson, K. M., Possell, M., Aspinwall, M. J., Pfautsch, S., and Tjoelker, M. G.: Temperature response measurements from eucalypts give insight into the impact of Australian isoprene emissions on air quality in 2050, Atmos. Chem. Phys., 20, 6193–6206, https://doi.org/10.5194/acp-20-6193-2020, 2020.

Erdogan, H. E., Pellikka, P. K. E., and Clark, B.: Modelling the impact of land-cover change on potential soil loss in the Taita Hills, Kenya, between 1987 and 2003 using remote-sensing and geospatial data. Int. J. Remote Sens., 32, 5919–
475   5945, https://doi.org/10.1080/01431161.2010.499379, 2011.

Faiola, C., and Taipale, D.: Impact of insect herbivory on plant stress volatile emissions from trees: a synthesis of quantitative measurements and recommendations for future research. Atmos. Environ. X 5, 100060. https://doi.org/10.1016/j.aeaoa.2019.100060, 2020.

Gierens, R.T., Laakso, L., Mogensen, D., Vakkari, V., Beukes, J. P., Van Zyl P. G., Hakola, H., Guenther, A., Pienaar, J.
480   J., and Boy, M.: Modelling new particle formation events in the South African savannah. South African Journal of Science, 110(5/6), 12, http://dx.doi.org/10.1590/ sajs.2014/20130108, 2014.

Gill, K. J. and Hites, R. A.: Rate Constants for the gas-phase reactions of the hydroxyl radical with isoprene, α- and β-pinene, and limonene as a function of temperature, J. Phys. Chem. A, 106, 2538-2544, https://doi.org/10.1021/jp013532q, 2002.

485 Grant, D. D., Fuentes, J. D., Chan, S., Stockwell, W. R., Wang, D., and Ndiaye, S. A.: Volatile organic compounds at a rural site in western Senegal, J. Atmos. Chem., 60, 19–35, 10.1007/s10874-008-9106-1, 2008.

Greenberg, J. P., Guenther, A., Zimmerman, P., Baugh, W., Geron, C., Davis, K., Helmig, D., and Klinger, L. F.: Tethered balloon measurements of biogenic VOCs in the atmospheric boundary layer, Atmos. Environ., 33, 855–867, https://doi.org/10.1016/S1352-2310(98)00302-1, 1999.

490 Greenberg J. P., Guenther, A., Harley, P., Otter, L., Veenendaal, E. M., Hewitt, C. N., James, A. E., and Owen, S. M.: Eddy flux and leaf-level measurements of biogenic VOC emissions from mopane woodland of Botswana. J. Geophys. Res. 108(D13), 8466, doi:10.1029 2002JD002317, 2003.

Greenberg, J. P., Asensio, D., Turnipsseed, A., Guenther, A., Karl T., and Gochis, D.: Contribution of leaf and needle litter to whole ecosystem BVOC fluxes, Atmospheric Environment, 59, 302–311,
495   https://doi.org/10.1016/j.atmosenv.2012.04.038, 2012.

Grosjean, E. and Grosjean, D.: Rate constants for the gas-phase reactions of ozone with unsaturated aliphatic alcohols, Int. J. Chem. Kinet., 26, 1185-1191, https://doi.org/10.1002/kin.550261206, 1994.

Guenther, A.: Biological and Chemical Diversity of Biogenic Volatile Organic Emissions into the Atmosphere, ISRN Atmos. Sci., 2013, 1–27, doi:10.1155/2013/786290, 2013.

500 Guenther, A. B., Monson, R. K., and Fall, R.: Isoprene and monoterpene emission rate variability: Observations with eucalyptus and Emission Rate Algorithm Development, J. Geophys. Res., 96, 10 799–10 808, https://doi.org/10.1029/91JD00960, 1991.

Guenther, A. B., Zimmerman, P. R., Harley, P. C., Monson, R. K., and Fall, R.: Isoprene and Monoterpene Emission Rate Variability – Model Evaluations and Sensitivity Analyses, J. Geophys. Res. Atmos., 98(D7), 12 609–12 617,
505   https://doi.org/10.1029/93JD00527, 1993.

Guenther, A., Otter, L., Zimmerman, P., Greenberg, J., Scholes, R., Scholes, M.: Biogenic hydrocarbon emissions from southern African savannas, J. Geophys. Res. Atmos., 101, 25859–25865, https://doi.org/10.1029/96JD02597, 1996.

Guenther, A. B., Jiang, X., Heald, C. L., Sakulyanontvittaya, T., Duhl, T., Emmons, L. K., and Wang, X.: The Model of Emissions of Gases and Aerosols from Nature version 2.1 (MEGAN2.1): an extended and updated framework for
510   modeling biogenic emissions, Geosci. Model Dev., 5, 1471–1492, https://doi.org/10.5194/gmd-5-1471-2012, 2012.

Hakola, H., Hellén, H., Hemmilä, M., Rinne, J., and Kulmala, M.: In situ measurements of volatile organic compounds in a boreal forest, Atmos. Chem. Phys., 12, 11665–11678, https://doi.org/10.5194/acp-12-11665-2012, 2012.

Harley, P., Otter, L., Guenther, A., and Greenberg, J.: Micrometeorological and leaf-level measurements of isoprene emissions from a southern African savanna. Journal of Geophysical Research, 108, doi 10.1029/2002JD002592, 2003.

Helin, A., Hakola, H., and Hellén, H.: Optimisation of a thermal desorption–gas chromatography–mass spectrometry method for the analysis of monoterpenes, sesquiterpenes and diterpenes, Atmos. Meas. Tech., 13, 3543–3560, https://doi.org/10.5194/amt-13-3543-2020, 2020.

Hellén, H., Praplan, A. P., Tykkä, T., Ylivinkka, I., Vakkari, V., Bäck, J., Petäjä, T., Kulmala, M., and Hakola, H.: Long-term measurements of volatile organic compounds highlight the importance of sesquiterpenes for the atmospheric chemistry of a boreal forest, Atmos. Chem. Phys., 18, 13839–13863, https://doi.org/10.5194/acp-18-13839-2018, 2018.

Holopainen, J. K., Gershenzon, J.: Multiple stress factors and the emission of plant VOCs. Trends Plant Sci., 15, 176–184, https://doi.org/10.1016/j.tplants.2010.01.006, 2010.

Hüve K., Christ. M. M., Kleist, E., Uerlings, R., Niinemets, Ü., Walter, A., and Wildt, J.: Simultaneous growth and emission measurements demonstrate an interactive control of methanol release by leaf expansion and stomata, J. Exp. Bot., 58, 1783–1793, doi: 10.1093/jxb/erm038, 2007.

IPCC: Climate Change 2014: Impacts, Adaptation and Vulnerability. Contribution of Working Group II to the Fourth Assessment Report of the Intergovernmental Panel on Climate Change, Cambridge University Press, Cambridge, UK, 2014.

Jaars, K., Van Zyl, P. G., Beukes, J. P., Hellén, H., Vakkari, V., Josipovic, M., Venter, A. D., Räsänen, M., Knoetze, L., Cilliers D. P., Siebert, S. J., Kulmala, M., Rinne, J., Guenther, A., Laakso, L., and Hakola, H.: Measurements of biogenic volatile organic compounds at a grazed savannah grassland agricultural landscape in South Africa, Atmos. Chem. Phys., 16(24), 15665–15688, https://doi.org/10.5194/acp–16–15665–2016, 2016.

Jardine, A. B., Jardine, K. J., Fuentes, J. D., Martin, S. T., Martins, G., Durgante, F., Carneiro, V., Higuchi, N., Manzi, A. O., and Chambers, J. Q.: Highly reactive light-dependent monoterpenes in the Amazon, Geophys. Res. Lett., 42, 1576–1583, https://doi.org/10.1002/2014GL062573, 2015.

Jenkin, M. E., Saunders, S. M., and Pilling, M. J.: The tropospheric degradation of volatile organic compounds: a protocol for mechanism development, Atmos. Environ., 31, 81-104, https://doi.org/10.1016/S1352-2310(96)00105-7, 1997.

Kharin, V., Flato, G. M, Zhang, X., Gillett, N. P., Zwiers, F., and Anderson, K. J.: Risks from Climate Extremes Change Differently from 1.5°C to 2.0°C Depending on Rarity, Earth's Future, 6(5), 704–715, doi:10.1002/2018ef000813, 2018.

Kleindienst, T. E., Harris, G. W., and Pitts Jr., J. N.: Rates and temperature dependences of the reaction of hydroxyl radical with isoprene, its oxidation products, and selected terpenes, Environ. Sci. Technol., 16, 844-846, https://doi.org/10.1021/es00106a004, 1982.

Klinger, L. F., Greenburg J., Guenther, A., Tyndall, G., Zimmerman, P., M'Bangui, M., Moutsamboté, J. M., Kenfack, D.: Patterns in volatile organic compound emissions along a savanna-rainforest gradient in central Africa, J. Geophys. Res. Atmos., 103, 1443-1454, https://doi.org/10.1029/97JD02928, 1998.

Kulmala, M., Suni, T., Lehtinen, K. E. J., Dal Maso, M., Boy, M., Reissell, A., Rannik, Ü., Aalto, P., Keronen, P., Hakola, H., Bäck, J., Hoffmann, T., Vesala, T., and Hari, P.: A new feedback mechanism linking forests, aerosols, and climate, Atmos. Chem. Phys., 4, 557–562, https://doi.org/10.5194/acp-4-557-2004, 2004.

LAI, https://land.copernicus.eu/global/products/lai, last access: 12/14/2020.

Liu, Y., Schallhart, S., Tykkä, T., Räsänen, M., Merbold, L., Hellén, H., and Pellikka, P.: Biogenic volatile organic compounds in different ecosystems in southern Kenya. Atmos. Environ., 246, 118064,
555 https://doi.org/10.1016/j.atmosenv.2020.118064, 2021.

Loreto F., Förster A., Durr M., Csiky O., and Seufert G.: On the monoterpene emission under heat stress and on the increased thermotolerance of leaves of Quercus ilex L. fumigated with selected monoterpenes, Plant Cell Environ., 21, 101-107, https://doi.org/10.1046/j.1365-3040.1998.00268.x, 1998.

Masui, N., Agathokleous, E., Mochizuki, T., Tani, A., Matsuura, T., Koike, T.: Ozone disrupts the communication
560 between plants and insects in urban and suburban areas: an updated insight on plant volatiles, J. For. Res., https://doi.org/10.1007/s11676-020-01287-4, 2021.

Matsunaga, S. N., Wiedinmyer, C., Guenther, A. B., Orlando, J. J., Karl, T., Toohey, D. W., Greenberg, J. P., and Kajii, Y.: Isoprene oxidation products are a significant atmospheric aerosol component, Atmos. Chem. Phys. Discuss., 5, 11143–11156, https://doi.org/10.5194/acpd-5-11143-2005, 2005.

565 MDAUS BaseVue 2013, https://www.africageoportal.com/datasets/b4a808eba17d4294991880d9e120faee, last access: 15 December, 2020.

Mochizuki, T., Ikeda, F., and Tani, A.: Effect of growth temperature on monoterpene emission rates of Acer palmatum, Science of the Total Environment, 745, 140886, https://doi.org/10.1016/j.scitotenv.2020.140886, 2020.

Mogensen, D., Smolander, S., Sogachev, A., Zhou, L., Sinha, V., Guenther, A., Williams, J., Nieminen, T., Kajos, M. K.,
570 Rinne, J., Kulmala, M., and Boy, M.: Modelling atmospheric OH-reactivity in a boreal forest ecosystem, Atmos. Chem. Phys., 11, 9709–9719, https://doi.org/10.5194/acp-11-9709-2011, 2011.

Mogensen, D., Gierens, R., Crowley, J. N., Keronen, P., Smolander, S., Sogachev, A., Nölscher, A. C., Zhou, L., Kulmala, M., Tang, M. J., Williams, J., and Boy, M.: Simulations of atmospheric OH, O3 and NO3 reactivities within and above the boreal forest, Atmos. Chem. Phys., 15, 3909–3932, https://doi.org/10.5194/acp–15–3909–2015, 2015.

575 Mutzel, A., Poulain, L., Berndt, T., Iinuma, Y., Rodigast, M., Böge, O., Richters, S., Spindler, G., Sipilä, M., Jokinen, T., Kulmala, M., and Herrmann, H.: Highly oxidized multifunctional organic compounds observed in tropospheric particles: a field and laboratory study, Environ. Sci. Technol., 49, 7754–7761, https://doi.org/10.1021/acs.est.5b00885, 2015.

Ng, N. L., Brown, S. S., Archibald, A. T., Atlas, E., Cohen, R. C., Crowley, J. N., Day, D. A., Donahue, N. M., Fry, J.
580 L., Fuchs, H., Griffin, R. J., Guzman, M. I., Herrmann, H., Hodzic, A., Iinuma, Y., Jimenez, J. L., Kiendler-Scharr, A., Lee, B. H., Luecken, D. J., Mao, J., McLaren, R., Mutzel, A., Osthoff, H. D., Ouyang, B., Picquet-Varrault, B., Platt, U., Pye, H. O. T., Rudich, Y., Schwantes, R. H., Shiraiwa, M., Stutz, J., Thornton, J. A., Tilgner, A., Williams, B. J., and Zaveri, R. A.: Nitrate radicals and biogenic volatile organic compounds: oxidation, mechanisms, and organic aerosol, Atmos. Chem. Phys., 17, 2103–2162, https://doi.org/10.5194/acp-17-2103-2017, 2017.

585 Niang, I., Ruppel, O. C., Abdrabo, M. A., Essel, A., Lennard, C., Padgham, J., and Urquhart, P.: Africa. In: Climate Change 2014: Impacts, Adaptation, and Vulnerability. Part B: Regional Aspects. Contribution of Working Group II to the Fifth Assessment Report of the Intergovernmental Panel on Climate Change [Barros, V. R., Field, C. B., Dokken, D. J., Mastrandrea, M. D., Mach, K. J., Bilir, T. E., Chatterjee, M., Ebi, K. L., Estrada, Y. O., Genova, R. C., Girma, B., Kissel, E. S., Levy, A. N., MacCracken, S., Mastrandrea, P. R., and White, L. L. (eds.)]. Cambridge
590 University Press, Cambridge, United Kingdom and New York, NY, USA, 1199–1265, 2014.

Niinemets U, Loreto F, and Reichstein M.: Physiological and physico–chemical controls on foliar volatile organic compound emissions. Trends Plant Sci 9:180–186, DOI: 10.1016/j.tplants.2004.02.006. 2004.

Niinemets U.: Mild versus severe stress and BVOCs: thresholds, priming and consequences. Trends Plant Sci., 15, 145–153, https://doi.org/10.1016/j.tplants.2009.11.008, 2010.

595 Otter, L. B., Guenther, A., and Greenberg, J.: Seasonal and spatial variations in biogenic hydrocarbon emissions from southern African savannas and woodlands, Atmos. Environ., 36, 4265–4275, doi:10.1016/S1352–2310(02)00333–3, 2002.

Pellikka, P., Lötjönen, M., Siljander, M., and Lens, L.: Airborne remote sensing of spatiotemporal change (1955–2004) in indigenous and exotic forest cover in the Taita Hills, Kenya, INT J APPL EARTH OBS, 11(4), 221–232, doi: 600 10.1016/j.jag.2009.02.002, 2009.

Pellikka, P. K. E., Heikinheimo, V., Hietanen, J., Schäfer, E., Siljander, M., and Heiskanen, J.: Impact of Land Cover Change on Aboveground Carbon Stocks in Afromontane Landscape in Kenya, Appl. Geogr., 94, 178–189, https://doi.org/10.1016/j.apgeog.2018.03.017, 2018.

Peñuelas, J., and Staudt, M. BVOCs and global change. Trends in Plant Science, 15(3), 133–144. 605 https://doi.org/10.1016/j.tplants.2009.12.005, 2010.

Petäjä, T., Mauldin, III, R. L., Kosciuch, E., McGrath, J., Nieminen, T., Paasonen, P., Boy, M., Adamov, A., Kotiaho, T., and Kulmala, M.: Sulfuric acid and OH concentrations in a boreal forest site, Atmos. Chem. Phys., 9, 7435–7448, doi:10.5194/acp–9–7435–2009, 2009.

Rohrer, F. and Berresheim, H.: Strong correlation between levels of tropospheric hydroxyl radicals and solar ultraviolet 610 radiation, Nature, 442, 184–187, https://doi.org/10.1038/nature04924, 2006.

Rudich, Y., Talukdar, R. K., Burkholder, J. B., and Ravishankara, A. R.: Reaction of methylbutenol with the OH radical: Mechanism and atmospheric implications, J. Phys. Chem., 99, 12188-12194, https://doi.org/10.1021/j100032a021, 1995.

Räsänen, M., Merbold, L., Vakkari, V., Aurela, M., Laakso, L., Beukes, J.P., Van Zyl, P.G., Josipovic, M., Feig, G., 615 Pellikka, P., Rinne, J., and Katul, G.: Root–zone soil Moisture variability across African savannas: From pulsed rainfall to landcover switches. Ecohydrology, e2213, https://doi.org/10.1002/eco.2213, 2020.

Saunders, S. M., Jenkin, M. E., Derwent, R. G., and Pilling, M. J.: Protocol for the development of the Master Chemical Mechanism, MCM v3 (Part A): tropospheric degradation of non-aromatic volatile organic compounds, Atmos. Chem. Phys., 3, 161–180, https://doi.org/10.5194/acp-3-161-2003, 2003.

620 Saxton, J. E., Lewis, A. C., Kettlewell, J. H., Ozel, M. Z., Gogus, F., Boni, Y., Korogone, S. O. U., and Serça, D.: Isoprene and monoterpene measurements in a secondary forest in northern Benin, Atmos. Chem. Phys., 7, 4095–4106, doi:10.5194/acp–7–4095–2007, 2007.

Schade, G. W., Goldstein, A. H., and Lamanna, M. S.: Are monoterpene emissions influenced by humidity? Geophysical Research Letters 26(14), 2187–2190, https://doi.org/10.1029/1999GL900444, 1999.

625 Schulze, B. C., Wallace, H. W., Flynn, J. H., Lefer, B. L., Erickson, M. H., Jobson, B. T., Dusanter, S., Griffith, S. M., Hansen, R. F., Stevens, P. S., VanReken, T., and Griffin, R. J.: Differences in BVOC oxidation and SOA formation above and below the forest canopy, Atmos. Chem. Phys., 17, 1805–1828, https://doi.org/10.5194/acp–17–1805–2017, 2017.

Seneviratne, S. I., Nicholls, N., Easterling, D., Goodess, C. M., Kanae, S., Kossin, J., Luo, Y., Marengo, J., McInnes, K., 630 Rahimi, M., Reichstein, M., Sorteberg, A., Vera, C., and Zhang, X.: Changes in climate extremes and their impacts on the natural physical environment. In: Managing the Risks of Extreme Events and Disasters to Advance Climate Change Adaptation [Field, C. B., Barros, V., Stocker, T.F., Qin, D., Dokken, D. J., Ebi, K. L., Mastrandrea, M. D.,

Mach, K. J., Plattner, G. K., Allen, S. K., Tignor, M., Midgley, P. M. (eds.)]. A Special Report of Working Groups I and II of the Intergovernmental Panel on Climate Change (IPCC). Cambridge University Press, Cambridge, UK, and New York, NY, USA, 109–230, 2012.

635

Serça, D., Guenther, A., Klinger, L., Vierling, L., Harley, P., Druilhet, A., Greenberg, J., Baker, B., Baugh, W., and Bouka-Biona, C.: EXPRESSO flux measurements at upland and lowland Congo tropical forest site, Tellus B, 53, 220–234, https://doi.org/10.3402/tellusb.v53i3.16593, 2001.

Shu, Y. and Atkinson, R.: Rate constants for the gas-phase reactions of O3 with a series of terpenes and OH radical

640   formation from the O3 reactions with Sesquiterpenes at 296 ± 2 K, Int. J. Chem. Kinet., 26, 1193-1205, https://doi.org/10.1002/kin.550261207, 1994.

Simpson, D. Winiwarter, W., Börjesson, G., Cinderby, S., Ferreiro, A., Guenther, A., Hewitt, C. N., Janson, R., Aslam K. Khalil, M., Owen, S., Pierce, T. E., Puxbaum, H., Shearer, M., Skiba, U., Steinbrecher, R., Tarrasón, L., and Öquist, M. G.: Inventorying emissions from Nature in Europe, J. Geophys. Res. A, 104, 8113–8152,

645   https://doi.org/10.1029/98JD02747, 1999.

Simpson, D., Benedictow, A., Berge, H., Bergström, R., Emberson, L. D., Fagerli, H., Flechard, C. R., Hayman, G. D., Gauss, M., Jonson, J. E., Jenkin, M. E., Nyíri, A., Richter, C., Semeena, V. S., Tsyro, S., Tuovinen, J. P., Valdebenito, Á., and Wind, P.: The EMEP MSC-W chemical transport model – technical description, Atmos. Chem. Phys., 12, 7825–7865, https://doi.org/10.5194/acp-12-7825-2012, 2012.

650 Sporre, M. K., Blichner, S. M., Karset, I. H. H., Makkonen, R., and Berntsen, T. K.: BVOC–aerosol–climate feedbacks investigated using NorESM, Atmos. Chem. Phys., 19, 4763–4782, https://doi.org/10.5194/acp-19-4763-2019, 2019.

Stone, D., Evans, M. J., Commane, R., Ingham, T., Floquet, C. F. A., McQuaid, J. B., Brookes, D. M., Monks, P. S., Purvis, R., Hamilton, J. F., Hopkins, J., Lee, J., Lewis, A. C., Stewart, D., Murphy, J. G., Mills, G., Oram, D., Reeves, C. E., and Heard, D. E.: HOx observations over West Africa during AMMA: impact of isoprene and NOx, Atmos.

655   Chem. Phys., 10, 9415–9429, https://doi.org/10.5194/acp-10-9415-2010, 2010.

Taipale, D., Aalto, J., Schiestl-Aalto, P., Kulmala, M., and Bäck, J. The importance of accounting for enhanced emissions of monoterpenes from new Scots pine foliage in models - A Finnish case study. Atmos. Environ. X, 100097, doi:10.1016/j.aeaoa.2020.100097, 2020.

Unger, N.: Human land–use–driven reduction of forest volatiles cools global climate, Nature Climate Change, 4(10),

660   907–910, https://doi.org/10.1038/nclimate2347, 2014.

Velikova, V. B.: Isoprene as a tool for plant protection against abiotic stresses, Journal of Plant Interactions, 3, 1-15, doi: 10.1080/17429140701858327, 2008.

Vilà-Guerau de Arellano, C. C. van Heerwaarden, B. J. van Stratum, and K. van den Dries: Atmospheric Boundary Layer: Integrating Air Chemistry and Land Interactions. Cambridge University Press, doi:10.1017/CBO9781316117422,

665   2015.

Wachiye S., Merbold L., Vesala T., Rinne J., Räsänen M., Leitner S., and Pellikka P.: Soil greenhouse gas emissions under different land-use types in savanna ecosystems of Kenya. Biogeosciences, 17, 2049–2167, https://doi.org/10.5194/bg-17-2149-2020, 2020.

WDC: The World Data Center for Remote Sensing of the Atmosphere:

670   http://wdc.dlr.de/data_products/SERVICES/PROMOTE_O3/vmr.html, last access: December 15th, 2020.

Wildermuth, M. C., and Fall, R.: Light-dependent isoprene emission (Characterization of a thylakoid-bound isoprene synthase in Salix discolor chloroplasts), Plant Physiol., 112, 171–182, https://doi.org/10.1104/pp.112.1.171, 1996.

Wright, G. A., Lutmerding, A., Dudareva, N., and Smith, B. H.: Intensity and the ratios of compounds in the scent of snapdragon flowers affect scent discrimination by honeybees (Apis mellifera). J Comp Physiol A, 191, 105–114,

675   https://doi.org/10.1007/s00359-004-0576-6, 2005.

Zabel, F., Delzeit, R., Schneider, J., Seppelt, R., Mauser, W., and Václavík, T.: Global impacts of future cropland expansion and intensification on agricultural markets and biodiversity. Nat Commun, 10, 2844, https://doi.org/10.1038/s41467-019-10775-z, 2019.